Energy Distribution of Secondary Electrons from Copper-Beryllium Alloy by Positive Ions of Inert Gases. I. Electro-polished Surface

By Toshio SUGIURA

(Received January 17, 1961)

A series of studies of electron ejection from copper-beryllium (4%) alloy by positive ions have been extended in this work. In a previous paper[1], the yields of the secondary electron emission from the variously treated copper-beryllium targets by inert gas ions and some hydrocarbons and their fragment ions were measured, and the surface composition of these alloy targets were also determined by electron diffraction analysis in order to discuss the correlation between the yields of the secondary electron emission and the surface composition of the ion targets.

The secondary electron emission by inert gas ions had been studied by Hagstrum[2-6] on the atomically clean surfaces of some transition metals. The energy distribution of the secondary electrons ejected by the Auger process obeying the assumed mechanism had been theoretically calculated by Hagstrum[7], and a good agreement had been obtained between the theory and his experimental results.

Generally, the ejection of secondary electrons from a metal surface by impact of a positive ion proceeds at the expense of the potential or kinetic energy of the incident ion. Potential ejection may take place only if the ionization potential of the incident ion exceeds twice the work function of the target metal. Kinetic ejection, on the other hand, is expected to increase with increasing ion energy, and is the dominant process for all ions with kinetic energy above a few thousand electron volts, and it also proceeds for positive ions whose ionization potential is less than twice that of the work function of the metal.

Recently, Waters[8] had intended to confirm this kinetic ejection, and had measured the kinetic energy distribution of the ejected electrons from the atomically clean surface of tungsten impacted by alkali ions.

Unfortunately, the theory of the kinetic ejection by the positive ion having low kinetic energy had not yet been clarified, but the mechanism of secondary electron emission by the impact of high speed ions had been made the analysis by Sternglass[9]. He had studied the process of secondary electron emission regarded as the component of two essentially important parts, namely the formation of secondaries inside the metal and their subsequent escape from the surface. Also he had postulated that the energy loss of the primary particle as a result of the excitation and ionization of the target materials results in the formation of internal secondary electrons, and that the secondaries formed might lose their energy by various collison processes so that only a fraction of them may be able to reach the surface of the metal with sufficient energy to escape from the surface. The assumption of Sternglass seems to be suggestive for the secondary electron emission from the practical (not atomically clean) surfaces by impact of the ions.

The main points of interest of the present work are the direct measurements of the kinetic energy distribution of the secondary electrons ejected from the practical surface usable as the first dynode of the secondary electron multiplier tube, and the confirmation of the correlation between the yield of the secondary electron emission and the energy distribution of the secondary electron emission and the energy distribution of the secondary electrons. The results reported in this paper are concerned with the energy distribution of the secondary electrons ejected from the electro-polished copper-beryllium surface by impact of the singly- and doubly-charged argon and neon ions and singly-charged herium ions, together with the influence of the kinetic energy of these incident ions.

Experimental

In the experimentals of the electron ejection, the beam of ions which is homogeneous in constitution and kinetic energy was allowed to impinge upon a target surface. In order to measure the yield of secondary electrons (γ_1, number of electrons per incident ion) and the distribution in kinetic energy

1) T. Hayakawa and T. Sugiura, This Bulletin, **34**, 58 (1961).
2) H. D. Hagstrum, *Rev. Sci. Instr.*, **24**, 1122 (1953).
3) H. D. Hagstrum, *Phys. Rev.*, **89**, 244 (1953).
4) H. D. Hagstrum, ibid., **91**, 543 (1953).
5) H. D. Hagstrum, ibid., **96**, 325 (1954).
6) H. D. Hagstrum, ibid., **104**, 317, 672, 1516 (1956).
7) H. D. Hagstrum, ibid., **96**, 336 (1954).
8) P. M. Waters, ibid., **109**, 1053 (1958); **111**, 1466 (1958).
9) E. J. Sternglass, ibid., **108**, 1 (1957).

of ejected electrons, both as functions of the ion and target and of the ion kinetic energy, the apparatus must incorporate an ion source, a mass analyzer, an arrangement of target and surrounding electron collector, and the means to vary the velocity of the ion beam while keeping it focused on the target.

Mass Spectrometer. — The present experiments were performed by a mass spectrometer constructed in our laboratory, and their details were already reported in the previous paper[1]. In this studies, in order to eliminate the influence of the fringing field of the analyzing magnet on the slow electrons, the magnetic shield composed of six sheets of soft iron plates of 1.0 mm. in thickness was attached to the middle part between the ion collector region and the analyzing magnet. By this shielding, the influence of the fringing field on the energy distribution of secondary electrons was considered negligible, as described below.

Ion Target and Electron Collector. — Since the measurements of the energy distribution of the ejected electrons were made by the retarding potential method, the target was made relatively small and placed at the center of the spherical electron collector.

The ion target and the electron collector designed for the study of energy distribution of secondary electrons are schematically shown in Figs. 1a and b. In Figs. 1a and b, T indicates the ion target box shaped from the copper-beryllium (4%) plate, and the front area of this box is 6×12 mm^2 and the target was mounted at the center of the spherical electron collector S by the steatite insulator. S was constructed by two pieces of the brass blocks fastened to each other and the inside of these brass blocks were spherically excavated, the diameter of this sphere is 27 mm., and the area of the ion entrance slit Ss is 10×3 mm^2. In order to minimize the tertiary electron emission by secondary electrons and the variation of the contact potential with contamination by adsorped gases, the inside surface of the electron collector was covered with evaporated gold films. C is the collector slit of 8×2 mm^2 in area and shaped from a molybudenum plate of 0.2 mm. in thickness, and B is the buffer slit of 10×5 mm^2 in area formed by a copper plate of 0.4 mm. in thickness. The tungsten filament F was prepared inside the ion target box for heating the ion target by electron bombardment, and the temperature of the ion target was measured by a nickel-palladium thermocouple Th.

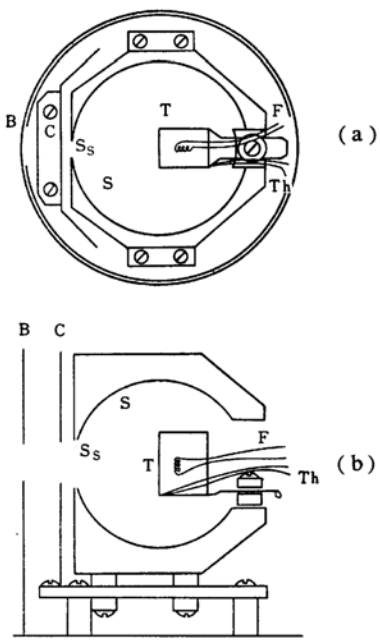

Fig. 1. Schematic top view (a) and side view (b) of the electron collector and ion target for the study of secondary electron emission by ion impact. T denotes the ion target, S the spherical electron collector, B, C and Ss the buffer, the collector and ion entrance slit, F the tungsten filament prepared for the heating of the ion target, Th the nickel-palladium thermocuple.

By these assemblies, all ions strike only the front surface of the ion target inside the spherical electron collector, since the focusing of the mass analyzer is determined by ion beam width less than 0.3 mm. at the collector slit during the course of studies.

Measurements of Energy Distributions of Secondary Electrons.—Electron energy distributions were measured in this work by means of the retarding potential method. Currents I_s at the electron collector were measured as a function of the voltage V_{sT} supplied between the ion target and the electron collector. The net ion currents I_i were measured by the ion target to which -18 V. was supplied against the electron collector through a battery in order to eliminate secondary electrons, and the ratio of the currents I_s/I_i was obtained as a function of the retarding potential V_{sT}.

Typical retarding potential data for the singly-charged argon ions are shown in Fig. 2. The kinetic energy distributions of the ejected electrons ($N_o(E_k)=d(I_s/I_i)/dV_r$) have been obtained from the retarding potential data in the following way where V_r denotes the retarding potential corrected to the contact potential difference between copper-beryllium and gold against V_{sT}. The differences in I_s/I_i for each 0.25 V. retarding potential difference was plotted vs. V_r. Typical energy distribution curves obtained from the data shown in Fig. 2 are shown in Fig. 3 in which the unit of $N_o(E_k)$ is electrons per ion per electron volt. A UX-54 tube was used as the primary tube of the d. c. amplifier, and the output current was recorded by two galvanometers of different sensitivities. Since a high resistance of 1×10^{10} ohm was used and the measured current was less than 1×10^{-11} amp. in all measurements, the inaccuracy of the retarding potential caused by the incident electrons or the primary ions is less than 0.1 V. and this causes no effective error in this study.

Measurement of Contact Potential Difference.— The apparatus used for the measurements of the contact potential difference is shown in Fig. 4a. The vacuum line of apparatus was all constructed

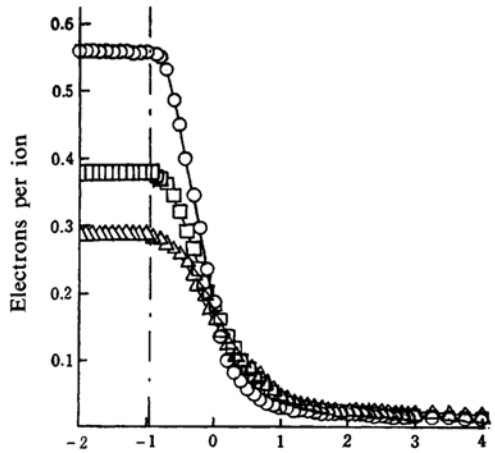

Fig. 2. Polt of ejected electron current I_s in electrons per ion as a function of the retarding potential V_{sT} for argon ions impinged on the electro-polished Cu-Be surface. Circule, square and triangle points denote impinged ion energy of 1240, 840 and 540 V., respectively.
The vertical line show on the electron energy scale indicates the contact potential difference between Au and electro-polished Cu-Be.

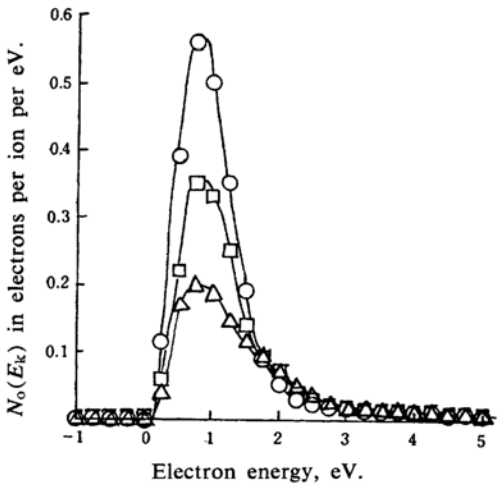

Fig. 3. Plot of the numbers of electrons per incident ion per eV. as a function of retarding potential V_r corrected for the contact potential difference. The curves plotted by circular, square and triangular points were obtained by differentiating the curves shown in Fig. 2.

by molybdenum glass and R in Fig. 4a is the measurement tube, and these were evacuated by the Hickman type oil diffusion pump through a liquid nitrogen trap, and the vacuum during the measurements was 1×10^{-6} mmHg. In Fig. 4b the electrode system is shown, the cylindrical electrode P was formed from a nickel plate of 0.2 mm. in thickness and the inside of this cylinder was covered

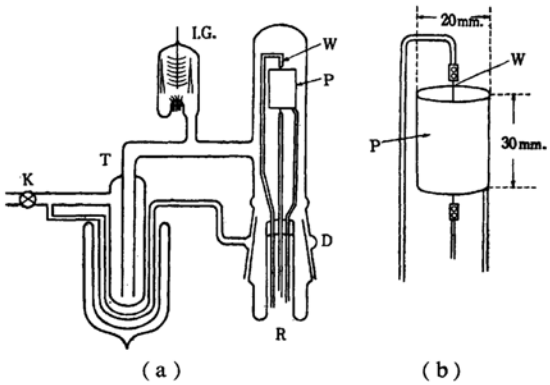

Fig. 4. Schematic diagram of the apparatus for the measurements of the contact potential difference (a). (b) show the electrode assembly. R denotes the measurement tube, P the retardation plate and the thermal electron collector, W the tungsten filament which supplying thermal electrons, I. G. the Bayard-Alpert ionization gauge, and T the liquid nitrogen trap.

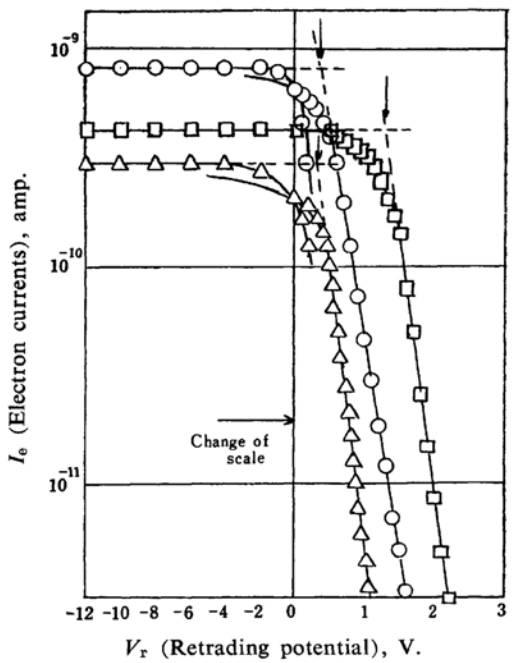

Fig. 5. Retarding potential data on thermoionic electron for the heated tungsten used to determine the contact potential difference between gold and electro-polished Cu-Be. The circle points show the Au—W system, the square points show the Cu-Be—W system, and the triangular points show the data of Hagstrum for Au—W system, in which the electron current scale is arbitrary for the Hagstrum's plot. The vertical arrow on each curve indicates the value for the zero field in each system.

with the evaporated gold film for the measurements of the contact potential difference between gold and tungsten, while for measurements of the contact potential difference between copper-beryllium and tungsten P was formed from a copper-beryllium plate of 0.15 mm. in thickness and was treated in the same manner as the ion target was. The tungsten filament F of 0.07 mm. in diameter was strung at the central axis of the electrode P. The electrode P and the tungsten filament F were mounted on a molybdenum rod in the measurement tube R. The geometry of the cylindrical electrode P was 20 mm. in inner diameter and 30 mm. in length. The stabilized 0.85 V. and 0.8 amp. were supplied to the filament in order to minimize the positive ion emission from the filament, the ionization of the residual gases and the photon radiation. Under these conditions, the thermal electron current of about 10^{-9} amp. was measured by a $\mu\mu$ ammeter. The retarding potential for the thermal electrons was applied on the center of the filament potential to the electrode P by dividing the battery potential. Typical results of the retarding potential curves for the thermal electrons emitted from the tungsten filament onto the gold plate or the copper-beryllium plate are shown in Fig. 5.

Materials.—The copper-beryllium ion target was shaped in a box-form after tempering and mechanical polishing with fine emery papers, and successively electro-polished in the solution which had been reported in the previous paper[1]. Spectroscopically pure argon and neon were used in the present experiments as well as in the previous sutdies, and also spectroscopically pure helium of the Teikoku Oxygen Co. was used without any further purifications. The mass spectrometric analyses of these gaseous samples revealed that the total impurities were less than 0.005% in volume.

Results

Contact Potential between Gold and Electro-polished Copper-Beryllium. — Typical retarding potential data obtained from the manner described above are shown in Fig. 5. In Fig. 5, the circle points indicate the retarding potential curve between the tungsten filament and the gold surface, while the square points show the retarding potential curve between tungsten filament and the electro-polished copper-beryllium surface. The triangle points in Fig. 5 indicate the results of the tungsten~gold system measured by Hagstrum[2] in which the electron current scale was shown in an arbitarary unit. As seen in Fig. 5, the retarding potential portion had been observed to be linear from 0.5 to 1.6 V. for the tungsten ~gold system, and to be linear from 1.4 to 2.2 V. for the tungsten~copper-beryllium system, while in Hagstrum's data the linear portion is from 0.5 to 1.1 V. The point of zero field has been determined by the intersection of the extrapolated straight lines through the saturated current and retarding portions as shown by arrows in each curve in Fig. 5.

These treatments of semilog plot are strictly correct only for plane parallel geometry[10], although the present author measured by geometry of cylindrical symmetry and Hagstrum[2] had measured by spherical geometry. But the present results of the tungsten—gold system are in close agreement with Hagstrum's result, and the discrepancies between these observed values and the true values are expected to be smaller than 0.1 V. The observed value of the contact potential difference between gold and electro-polished copper-beryllium alloy is 0.95 eV., while the surface potential of the electro-polished copper-beryllium is 0.95 eV. more positive than that of gold.

Kinetic Energy Distribution of Secondary Electrons. — The distribution curves of the kinetic energy of the secondary electron by singly- and doubly-charged argon and neon ions and by singly-charged herium ions are shown in Figs. 3, 6, 7, 8 and 9, respectively. In these figures the results obtained for the incident ion energies of 1240, 840 and 540 V. are respectively indicated by circles, squares and triangles, and the correction of the contact potential difference between the ion target and

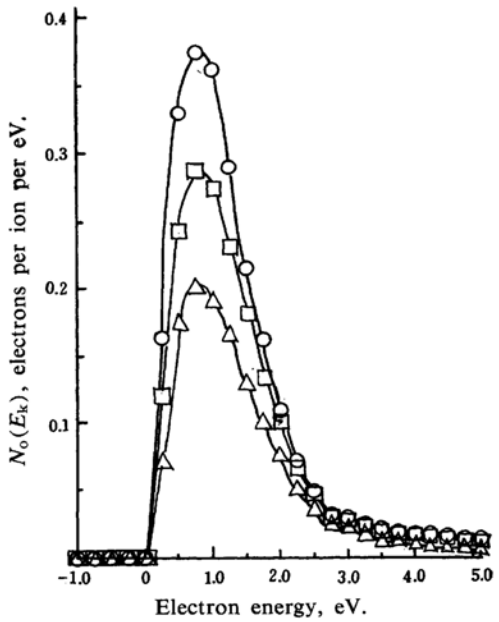

Fig. 6. Energy distributions of electron ejected from electro-polished Cu-Be by doubly-charged argon ions. Circular, square and triangular points denote the kinetic energy of incident ions of 1240, 840 and 540 V. respectively.

10) K. T. Compton and I. Langmuir, *Rev. Modern Phys.*, 3, 225 (1931).

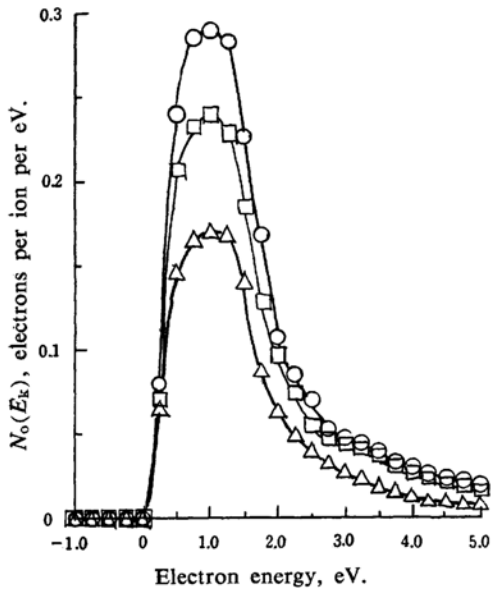

Fig. 7. Energy distributions of electron ejected from electro-polished Cu-Be by singly-charged neon ions. Circular, square and triangular points denote the kinetic energy of incident ions of 1240, 840 and 540 V. respectively.

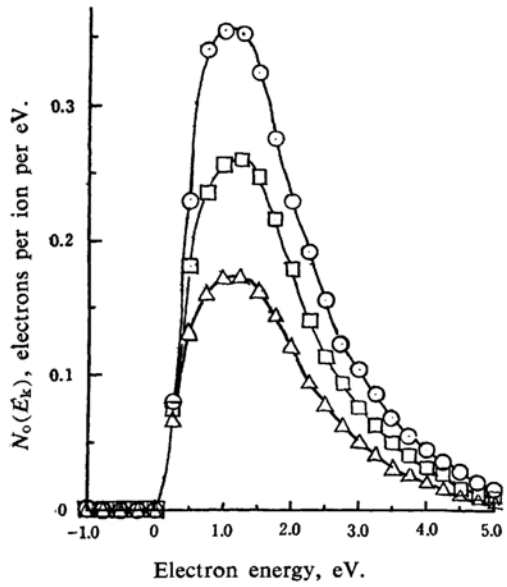

Fig. 8. Energy distributions of electron ejected from electro-polished Cu-Be by doubly-charged neon ions. Circular, square and triangular points denote the kinetic energy of incident ions of 1240, 840 and 540 V. respectively.

the electron collector was made for the retarding potential V_r.

These curves show that the fringing field of the analyzing magnet is negligible around the electron collector. If the fringing field is effective around the electron collector, then the electrons having low kinetic energy could not reach the electron collector and the distribution curves of the electron kinetic energy would have drifted to the low energy side. This effect has been studied by Hagstrum[3]. In the present studies, the magnetic field for the mass analyzer was varied for the focusing of ions having the various masses and kinetic energies, but every distribution curve obtained in this work practically showed that $N_0(E_k) = 0$ at the zero field in the retarding potential scale and no low energy tail has been observed.

The kinetic energy distribution shown by the half widths of each distribution curve and

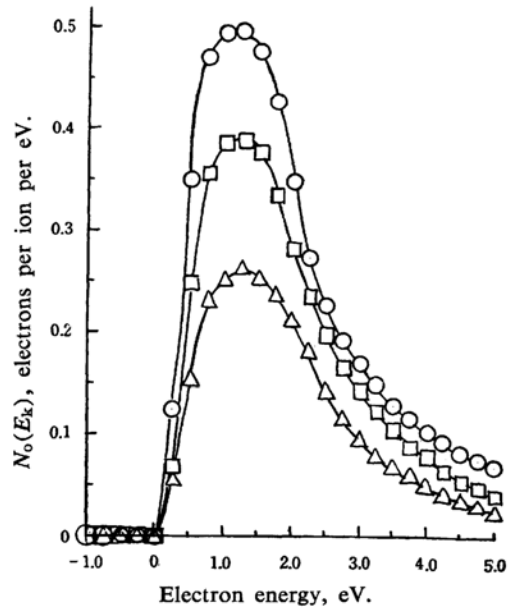

Fig. 9. Energy distributions of electron ejected from electro-polished Cu-Be by singly-charged herium ions. Circular, square and triangular points denote the kinetic energy of incident ions of 1240, 840 and 540 V. respectively.

TABLE I. VARIATION OF THE HALF WIDTHS OF THE ENERGY DISTRIBUTION CURVES AND YIELDS OF SECONDARY ELECTRONS FORM ELECTRO-POLISHED Cu-Be SURFACE WITH ION ENERGIES OF PRIMARY INERT GAS IONS

	Half widths of the energy distribution curves of secondary electrons in eV.			Yield of the secondary electrons γ_i in electrons per ion.		
Ion energy	1240	840	540	1240	840	540
Ion						
A^+	1.00	1.05	1.20	0.56	0.38	0.27
A^{2+}	1.30	1.35	1.40	0.58	0.43	0.36
Ne^+	1.40	1.45	1.50	0.57	0.43	0.31
Ne^{2+}	1.90	1.95	2.05	0.82	0.56	0.39
He^+	2.00	2.05	2.15	1.35	0.94	0.68

the yield γ_1 of the secondary electrons are summarized in Table I.

Discussion

General Features of Energy Distribution Curves.—As seen in Figs. 3, 6, 7, 8 and 9, all distribution curves have their maximum at about 1 eV. But the sharpness of each distribution curve is more similar to that of the lithium ions and the tungsten surface by Waters[8] than that of the argon ions and the tungsten surface by Hagstrum[6], both shown in Fig. 10. Although the surface in this work

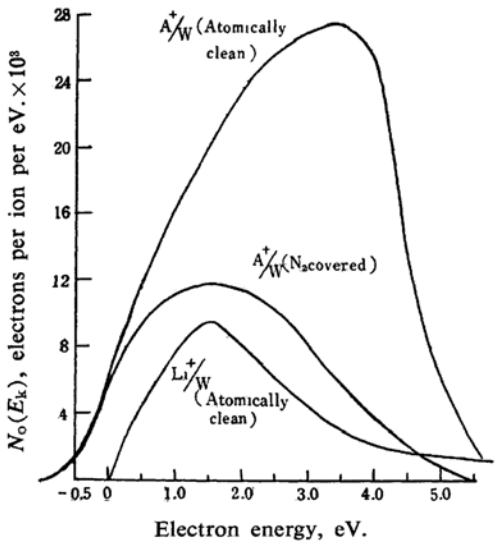

Fig. 10. Energy distributions of secondary electrons ejected by 10 eV. A^+ ions from atomically clean tungsten (W) and tungsten covered with the monolayer of nitrogen (N_2/W) given by Hagstrum[8], and the distribution curve of electron ejected by 1000 eV. Li^+ ions from atomically clean tungsten surface (Li^+) given by Waters[8].

was not atomically clean, the energy distribution curves observed in this work are not similar to that for the nitrogen covered surface of tungsten observed by Hagstrum shown in Fig. 10. The electron yields obtained in these studies are much greater than the results of Hagstrum and Waters. Since the present results were obtained from the alloy surface covered by residual gases and Hagstrum and Waters worked on the atomically clean surfaces of pure metals, the direct comparison of these data has no significant meaning, but the general features of the present distribution curves show much similarity of the kinetic ejection.

Effect of Ion Kinetic Energy.—As seen in Table I, the yield of the secondary electrons is clearly increased by increasing the kinetic energies of the incident ions, while the half width of the energy distribution curve of the secondary electrons is slightly decreased by increasing the ion kinetic energies. The difference between two distribution curves of different ion kinetic energies indicates the difference in the distribution of the different numbers of the secondary electrons emitted by different ion kinetic energies. In these different energy distributions, it is clearly shown that the increase in the electron yield as increasing the ion kinetic energies is mainly contributed to low energy electrons. This effect may be qualitatively explainable from the following idea similar to that of Sternglass[9]. Since the incident ions penetrate deeper as the ion kinetic energy increases, the number of secondary electrons formed in the alloy may be proportionally increased with the increase in the penetration depth. The formed secondary electrons may lose their energies in various types of collision processes, so that only a small fraction of them can reach the surface with sufficient energy to escape from the surface. But an increased number of electrons with the increase in the ion kinetic energy are formed in the deeper layer in the alloy, thus the detected secondary electrons might lose their initial energies during the passage through the layers in the alloy. The dependency of the distribution curves on the ion kinetic energy in these studies has previously been explained.

Influence of Ion Species.—As seen in Table I and Figs. 3, 7 and 9, the yield of the secondary electrons at any definite ion energy for the singly-charged inert gas ions is clearly increased in sequence from the argon, neon to helium ions, and this sequence has a correlation to their ionization potentials. Then, higher yield of the secondary electrons may be obtained by impact of the ion having the higher ionization potential.

As seen in Figs. 3, 7 and 9 and Table I, the energy distribution curves are broader for light ions than for heavier ions. These phenomena can not be explained by any similar explanation of the influence of the effect of the ion kinetic energy, since the ions of different masses are formed in the mass spectrometer with constant kinetic energy when the ions were accelerated by the acceleration voltage. If the penetration depth of the ions is assumed[9] to be simply dependent upon the ion kinetic energy, the penetration depth of the lighter ions is the same as that of the heavier ions. But the present results on the energy distribution clearly show the existence of the higher energy electrons in the case of lighter ions. They also indicate that the higher

energy electrons emitted by the ions have a higher ionization potential.

These phenomena indicate that the mechanism of the secondary electron ejection from the electro-polished copper-beryllium surface is not simple. The ionization potentials of argon, neon and helium are 15.76, 21.59 and 24.58 eV., respectively, and though the work function of the electro-polished copper-beryllium is not certain it may be presumed to be less than 6 eV. Then, it is considered from the present experimental conditions that the ionization potentials of the ions of the present consideration are larger then twice the work function of the alloy surface. Consequently, it remains open to discussion as to the mechanism of the potential ejection[7], but the general features of the distribution curves of the electron energies show considerable similarity to the kinetic ejection. For the reason mentioned above, it is difficult to deduce any simple conclusion on the mechanism of the electron emission by inert gas ions from the present work.

Effect of Ionic Charges.—From a comparison of Figs. 3 and 6 for argon ions and Figs. 7 and 8 for neon ions, the energy distribution curves by the doubly-charged ions are broader than those by the singly-charged ions, and the yield of the secondary electrons by the doubly-charged ions are greater than that by the singly-charged ions at any definite ion kinetic energy. Thus the energy distribution indicates that the doubly-charged ions ejected the higher energy electrons than the singly-charged ions do. This tendency is similar to the influence of the ion species on the yield and energy distribution of secondary electrons. The secondary ionization potential of the argon and neon ions are 43.52 and 62.57 eV., respectively, then the mechanism of the secondary electron emission from copper-beryllium may occur according to the complex mechanisms in which the secondary electron is ejected by contribution of both of the kinetic and the potential energies of the incident ions.

Summary

The distribution curves of the kinetic energies of the secondary electrons from the electro-polished copper-beryllium surface by inert gas ions were measured by the retarding potential method together with the yield of the secondary electron emission. The contact potential difference between the ion target (electro-polished copper-beryllium) and the electron collector (gold) was also measured by the retarding potential method for the thermal electrons from tungsten, and the correction of this contact potential difference was made for the kinetic energies of secondary electrons. The main results obtained are as follows.

(1) The contact potential difference between gold and electro-polished copper-beryllium (4%) is 0.95 eV. (gold, negative).

(2) The general features of the distribution curves of secondary electrons are similar to the distribution curves of the kinetic ejection measured by Waters.

(3) The present results of the energy distribution curves of secondary electrons by the inert gas ions indicate that the yield of secondary electrons is increased by increasing the kinetic energy of the primary ions, and that this increment in the yield is mainly contributed from the secondary electrons which have lower kinetic energies than that of the secondary electrons emitted by the incident ions of low kinetic energies. These phenomena are able to be postulated qualitatively by the idea of sternglass.

(4) The total number of emitted electrons is increased with the increase in the value of the ionization potential of incident ions, and the kinetic energies of emitted electrons become greater by increasing the potential energy of incident ions. These phenomena are difficult to explain by the mechanism of the kinetic ejection, therefore the electron emission from the electro-polished copper-beryllium surface by inert gas ions may occur according to the complicated mechanism in which the potential energies of incident ions contribute to the electron emission together with their kinetic energies.

(5) In contrast with the singly-charged ions, the doubly-charged ions give rise to the broadening of the energy distribution curves. This also suggests the occurrence of the comlicated ejection mechanisms.

The author wishes to acknowledge his indebtedness to Professor Shoji Shida of the Tokyo Institute of Technology, Professor Teruo Hayakawa and Professor Osamu Toyama of University of Osaka Prefecture, under whose direction and guidance this work was carried out.

The expense has been defrayed in part from a grant given by the Ministry of Education, to which the author's thanks are due.

Department of Applied Chemistry
Faculty of Engineering
University of Osaka Prefecture
Sakai, Osaka